Journal of Molecular Liquids 320 (2020) 114396

Contents lists available at ScienceDirect

Journal of Molecular Liquids

journal homepage: www.elsevier.com/locate/molliq

Rapid and sensitive detection of hypochlorite in ~100% aqueous solution using a bithiophene-based fluorescent sensor: Application to water analysis and live-cell imaging

Chunpeng Li, Pengcheng Yin, Tianduo Li, Tao Wei, Tingting Hu, Jianbin Chen, Xuyang Qin, Qingfen Niu *

Shandong Provincial Key Laboratory of Molecular Engineering, School of Chemistry and Chemical Engineering, Qilu University of Technology (Shandong Academy of Sciences), Jinan 250353, People's Republic of China

ARTICLE INFO

Article history:
Received 20 July 2020
Received in revised form 8 September 2020
Accepted 21 September 2020
Available online 28 September 2020

Keywords:
Fluorescent sensor
Hypochlorite
Water analysis
Bioimaging
Solid-state sensor

ABSTRACT

A new bithiophene-based biocompatible fluorescent and colorimetric sensor **2TD** capable of detecting hypochlorite (ClO^-) in enviro/biosystem was successfully synthesized. This sensor **2TD** underwent a highly specific and sensitive oxidation reaction with ClO^- and produced a bithiophene aldehyde (**2T-CHO**) emitting strong blue fluorescence, which was strongly confirmed by ^1H NMR, HRMS, FTIR and DFT calculation. The **2TD** for detecting ClO^- displays an ultra-fast response (25 s), great water-solubility (~100% aqueous solution), wide pH working range (7–11), excellent anti-interference capability, and ultra-sensitivity with low detection limit of 8.3 nM. Colorimetric test strips demonstrate that **2TD** can be utilized as a cost-effective and efficient solid-state sensor for rapidly and conveniently sensing ClO^- with great sensitivity in practical applications. With the robust applicability, the **2TD** was successfully utilized to determine/image ClO^- in environmental water and live-cells. More interestingly, this developed sensor **2TD** could be used as an efficient test tool for ClO^- sensing.

1. Introduction

Hypochlorite (ClO^-), as a vital reactive oxygen species (ROS) in living system, plays pivotal roles in various physi/pathological processes [1–7]. Research has found that biological ClO^- is mainly produced by oxygen during electron transfer process, which could not only act as a microbicidal mediator to kill many harmful pathogens and bacteria during the human immune defense process, but also is an indispensable disinfection in drinking water and household solutions widely used in our daily life [8–12]. However, the excessive ClO^- in living organisms can not only bring about oxidative stress and thus induced the oxidative damage via the oxidation of DNA, lipids as well as proteins, but also result in a number of serious inflammation-associated diseases such as atherosclerosis, arthritis, cardiovascular diseases, neuro degeneration and even cancer [2,13–18]. Presently, the recognizing and detecting ClO^- has become a challenging frontier in the development of chemistry. Hence, developing an efficient and convenient method for qualitative, quantitative, and sensitive detection of ClO^- in environmental and biological systems is of great significance.

Small fluorescent sensor is essential molecular tool and attracts much more attention for detecting ClO^-, in terms of its prominent advantages of high sensitivity, easiness of manipulating, real-time imaging, excellent spatial-temporal sampling capability for nondestructive detection [19–30]. To date, a great deal of ClO^--selective small fluorescent sensors have been developed [31–36]. However, to some extent, some previous sensors for sensing ClO^- are limited by fluorescence quenching, poor selectivity, slow response, and poor aqueous solubility, hampering their practical application for the real-time detection. Consequently, it is urgently needed to develop efficient fluorescent sensors for ultraselective, ultrasensitive and quantitative detection of ClO^- with excellent sensing properties and multiple applications.

In continuation to our interest on the development of fluorescent sensors for various analytes [37–51], in this study, a new bithiophene-diaminomaleonitrile-derived fluorescent sensor **2TD** has been synthesized (Scheme 1), which was used for the specific identification of ClO^- with fluorimetric-colorimetric dual-channel, ultrafast response, great aqueous solubility, excellent anti-interference capability, and ultrasensitivity in enviro/biosystem. Colorimetric test strips confirmed that **2TD** could be utilized as a cost-effective solid-state sensor for the rapid and convenient detection of ClO^- with great sensitivity in practical applications. Moreover, sensor **2TD** was not only successfully used to detect real environmental water sample analysis, but also utilized for bioimaging in living HeLa cells. Furthermore, the **2TD** served as a good fluorescent display material and the filter paper by letting **2TD** could be developed to prepare an ink-free writable paper by using ClO^- as the sole trigger.

* Corresponding author.
E-mail address: qf_niu1216@qlu.edu.cn (Q. Niu).

https://doi.org/10.1016/j.molliq.2020.114396
0167-7322/

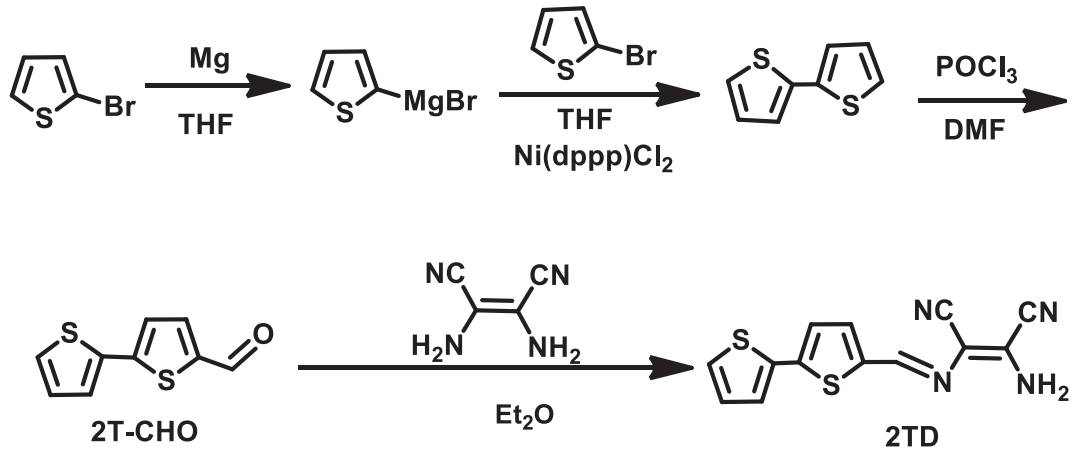

Scheme 1. The design and synthesis of sensor **2TD**.

2. Experimental section

2.1. Instruments and chemicals

The spectra of absorption, fluorescence, NMR, FTIR, and HRMS were completed by the spectrometer of Shimadzu UV-2600, Hitachi F-4600, Bruker AV-400, Bruker ALPHA FT-IR, and Q-TOF LC/MS Agilent 6510, respectively. The absolute fluorescence quantum yields (Φ_F) were obtained by an Edinburgh FLS1000 spectrophotometer. The pH value was determined by PHS-25 pH-meter. MTT assay was tested by microplate reader (Thermo Scientific, USA), and fluorescence images were obtained by confocal laser scanning microscope (CLSM) Leica TCS SP8 with a 63× magnification target oil lens. The DFT studies at the B3LYP/6-311G(d) level were performed via Gaussian 09 package. All the reagents involved in the experiments are analytically pure, which are purchased from commercial suppliers (Adamas, China) and were used directly. 2,2′-Bithiophene (2T) and [2,2′-bithiophene]-5-carbaldehyde (**2T-CHO**) were synthesized through the previous method [52,53]. The $ONOO^-$, ROO•, NO• and •OH were prepared according to the previous method [5,54]. Deionized water was used throughout the test process. For fluorescence measurements, the slits for excitation and emission were set at 5/5 nm, respectively, the voltage was set at 500 V, the scan rate was set at 2400 nm/min, and the excitation wavelength was set at 350 nm.

2.2. Synthesis of 2-(-([2,2′-bithiophen]-5-ylmethylene)amino)-3-aminomale-onitrile (*2TD*)

A mixture of compound **2T-CHO** (388 mg, 2.0 mmol) and diaminomaleonitrile (**DAMN**) (250 mg, 2.3 mmol) in dry EtOH (15 mL) was added catalytic amount of acetic acid glacial (2 drops). The above reaction mixture was stirred for 4 h under reflux. Upon completion, the orange precipitate was filtered-off, washed with ethanol and dried in vacuum to produce the final compound **2TD** (511 mg, yield: 90.1%). ^{1}H NMR (400 MHz, DMSO-d_6, ppm): δ = 8.40 (s, 1H), 7.77 (s, 2H), 7.72 (d, J = 4.0 Hz, 1H), 7.64 (d, J = 4.0 Hz, 1H), 7.45 (d, J = 4.0 Hz, 1H), 7.42 (d, J = 4.0 Hz, 1H), 7.16 (t, J = 4.0 Hz, 1H) (Fig. S1); ^{13}C NMR (100 MHz, DMSO-d_6, ppm): δ = 149.1, 142.4, 140.5, 135.6, 129.3, 127.7, 126.4, 126.0, 125.5, 115.0, 114.3, 103.4 (Fig. S2); FTIR (KBr, cm^{-1}): ν = 3455, 3306 (NH_2), 2207 (C≡N), 1600 (C=N) (Fig. S3); HRMS (ESI) m/z calcd for $C_{13}H_8N_4S_2$: 284.0190; Found: 285.0247, $[M+H]^+$ (Fig. S4).

2.3. Spectral measurements

A stock solution of sensor **2TD** (1 mM) was prepared in DMSO, and then the sensor **2TD** was diluted to 10 μM with ~100% aqueous solution (DMSO/H_2O, 1:99, v/v). Stock solutions (10 mM) of various anions (ClO^-, Br^-, F^-, Cl^-, ClO_4^-, HCO_3^-, CO_3^{2-}, PO_4^{3-}, SO_4^{2-}, NO_3^-, NO_2^-, $H_2PO_4^-$, HPO_4^{2-}, $S_2O_3^{2-}$, AcO^-), metal cations (Al^{3+}, Cr^{3+}, Fe^{3+}, Ni^{2+}, Pb^{2+}, Cu^{2+}, Hg^{2+}) and various reactive ROS or RNS species (H_2O_2, $ONOO^-$, •OH, •NO, ROO•) were dissolved in deionized water and used freshly. All spectroscopic measurements were measured at room temperature in ~100% aqueous solution (DMSO/H_2O, 1/99, v/v) with pH 7.

2.4. Cell incubation and fluorescence imaging

The HeLa cells were firstly seeded at a 96-well plate at 37 °C for 24 h, and then were treated with 10 μM sensor **2TD** for 60 min. After the cells being washed for 3 times with PBS buffer, and further incubated with 30 μM ClO^- for 30 min. Finally, the HeLa cell imaging was achieved by using CLSM under the 430–470 nm blue channel with an excitation at 405 nm.

3. Results and discussion

3.1. Selectivity and anti-interference studies

The sensor **2TD** itself is water-insoluble, the effect of solvent (different ratios between DMSO and H_2O) on the fluorescence spectra was firstly explored (Fig. S5), and the result indicated that the DMSO/H_2O (1/99, v/v) solution is the best detection media for all the sensing experiments. To evaluate the selectivity of sensor **2TD** to ClO^-, the absorption and fluorescence spectra of 10 μM **2TD** were performed upon treating with 20 μM various biological analytes in ~100% aqueous solution (DMSO/H_2O, 1/99, v/v). The anions including ClO^-, Br^-, F^-, Cl^-, ClO_4^-, HCO_3^-, CO_3^{2-}, PO_4^{3-}, SO_4^{2-}, NO_3^-, NO_2^-, $H_2PO_4^-$, HPO_4^{2-}, $S_2O_3^{2-}$, AcO^-, metal ions including (Al^{3+}, Cr^{3+}, Fe^{3+}, Ni^{2+}, Pb^{2+}, Cu^{2+}, Hg^{2+}), and reactive ROS or RNS species including H_2O_2, $ONOO^-$, •OH, ROO•, and •NO, were selected for the selectivity and competition tests, because some oxidizing and reducing species as well as some metal ions may have some effects on the sensor **2TD** through a redox or coordination reaction. As depicted in Fig. 1a, upon adding ClO^-, the main absorption peak at 378 nm disappeared, which was accompanied by a new absorption peak at 350 nm, with obvious yellow color change to colorless, while other tested analytes showed negligible response, suggesting that **2TD** had a highly specific selectivity for ClO^- over other tested species. Under the same conditions, the selectivity of the **2TD** towards ClO^- is further evaluated by fluorescence response. As displayed in Fig. 1b, the free **2TD** exhibited almost no fluorescence (Φ_F = 12.47%) after excitation at 350 nm, only the introduction of ClO^- resulted in a notable fluorescence enhancement at 423 nm (Φ_F = 20.09%) along with obvious fluorescence color change, indicating that **2TD** can effectively and selectively detect ClO^-.

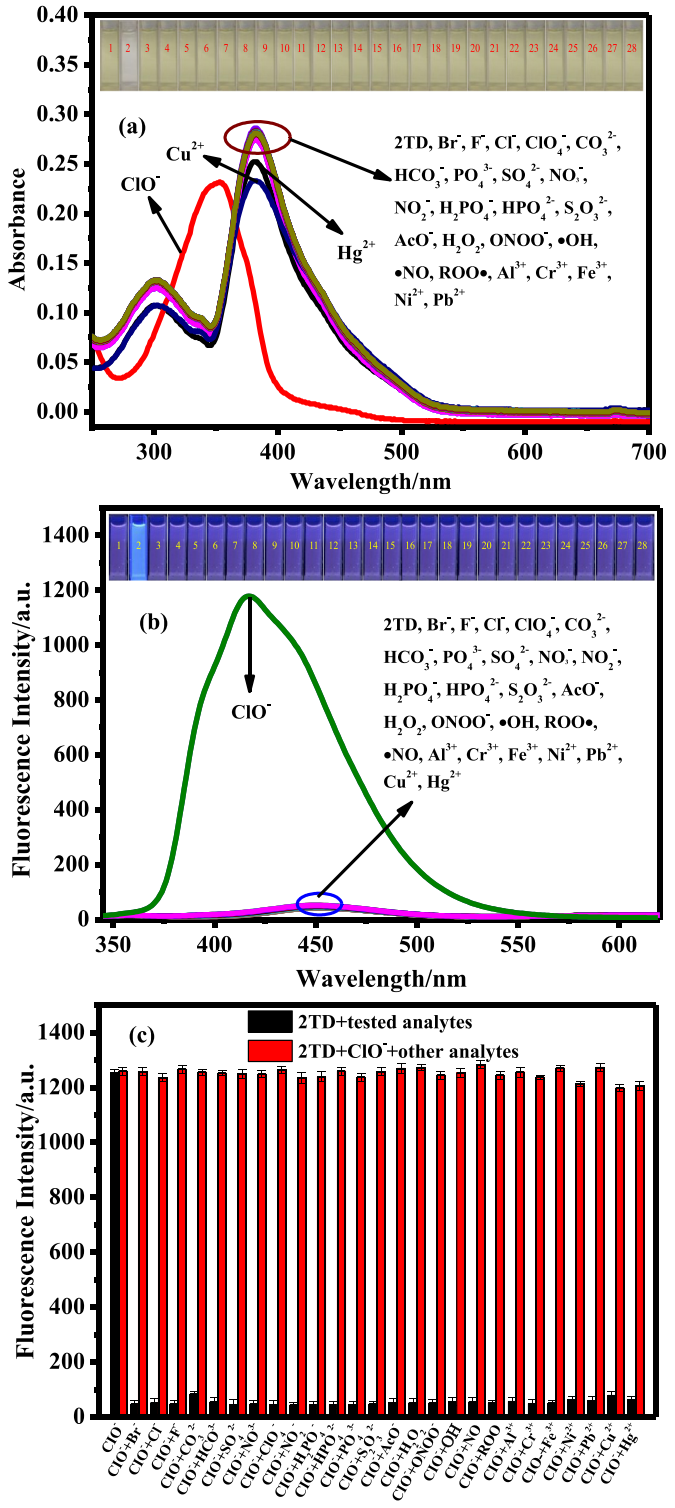

Fig. 1. (a) UV–Vis and (b) fluorescence spectral change of 10 μM **2TD** in ~100% aqueous media when treated with 20 μM tested analytes, insets: photographs showing visual color change for various tested analytes under sunlight and 365 illumination (1–28, free **2TD**, ClO^-, Br^-, F^-, Cl^-, ClO_4^-, CO_3^{2-}, HCO_3^-, PO_4^{3-}, SO_4^{2-}, NO_3^-, NO_2^-, $H_2PO_4^-$, HPO_4^{2-}, $S_2O_3^{2-}$, AcO^-, H_2O_2, $ONOO^-$, •OH, •NO, ROO•, Al^{3+}, Cr^{3+}, Fe^{3+}, Ni^{2+}, Pb^{2+}, Cu^{2+}, Hg^{2+}); (c) fluorescence intensity of **2TD** (10 μM) exposed to various analytes (100 μM) and to the mixture of ClO^- (100 μM) in ~100% aqueous solution (λ_{em} = 423 nm).

To verify whether many other environmentally and physiologically relevant analytes could cause interference for ClO^- detection and further confirm its specific selectivity in complex physiological environments, the competitive experiment was conducted by adding 10 equiv. of ClO^- to sensor **2TD** in the presence of 10 equiv. of other competitive active analytes, including common anions (ClO^-, Br^-, F^-, Cl^-, ClO_4^-, HCO_3^-, CO_3^{2-}, PO_4^{3-}, SO_4^{2-}, NO_3^-, NO_2^-, $H_2PO_4^-$, HPO_4^{2-}, $S_2O_3^{2-}$, AcO^-), metal cations (Al^{3+}, Cr^{3+}, Fe^{3+}, Ni^{2+}, Pb^{2+}, Cu^{2+}, Hg^{2+}) and reactive ROS or RNS species (H_2O_2, $ONOO^-$, •OH, ROO• and •NO) [55]. As displayed in Fig. 1c, a dramatic fluorescence intensity enhancement at 423 nm

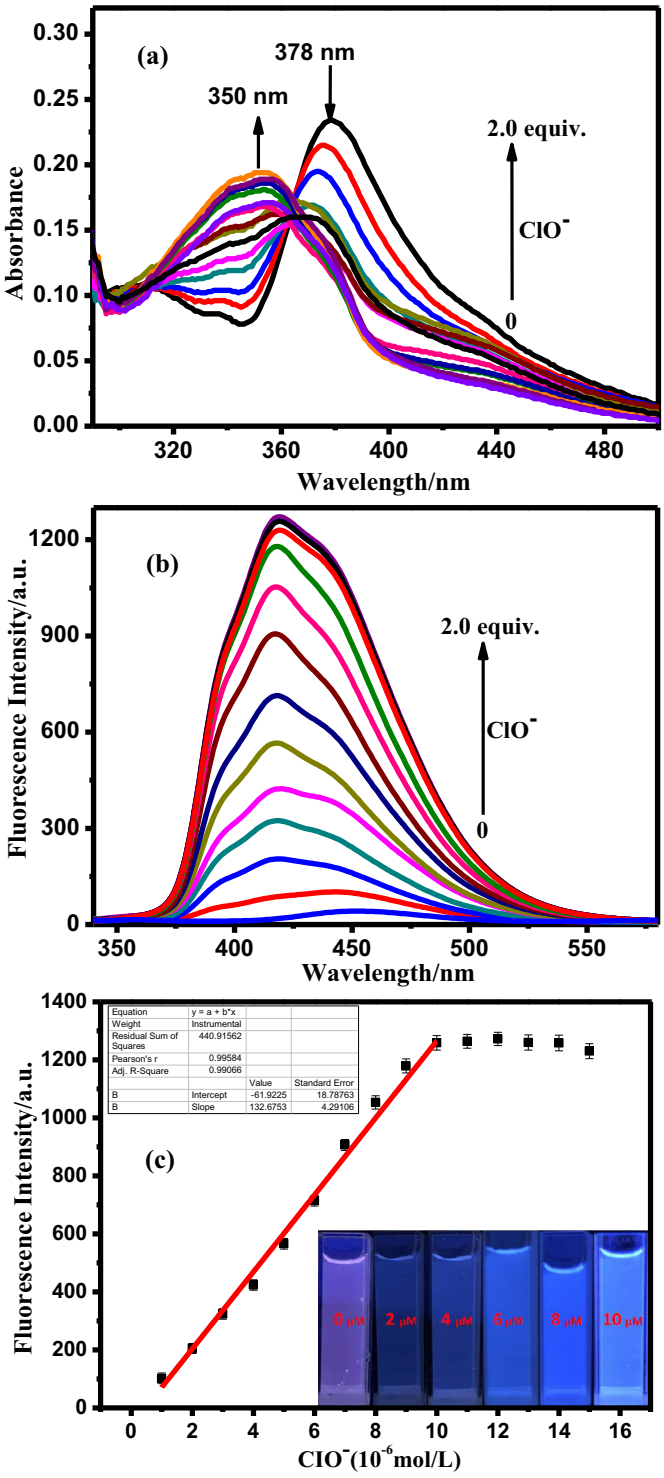

Fig. 2. Absorption (a) and fluorescence (b) spectral changes of 10 μM **2TD** in ~100% aqueous solution towards various ClO^- concentrations (0–20 μM); (c) the visual fluorescence variation of 10 μM **2TD** in ~100% aqueous solution with an increasing of ClO^- concentration.

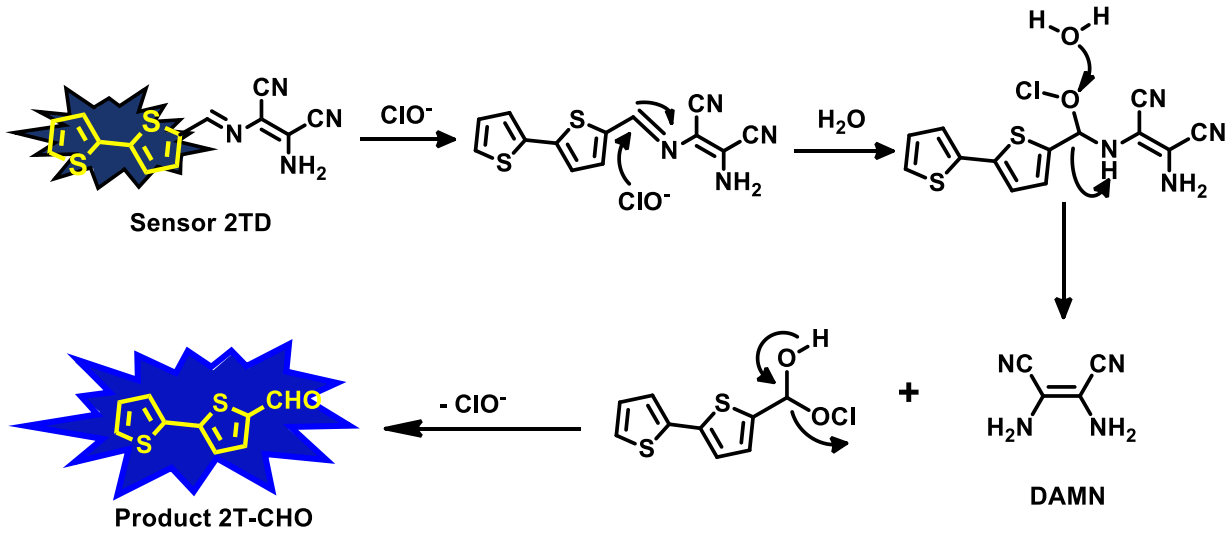

Scheme 2. The proposed mechanism of the sensor **2TD** sensing ClO^-.

occurred after treating with ClO^- coexisting with other various potentially interfering substances, and almost no remarkable fluorescence change was observed when other bio-active analytes coexisted. Thus, these results demonstrated that sensor **2TD** has good capable of anti-interference capability, and could be utilized to detect ClO^- in a competitive environment.

3.2. ClO^- sensing properties

To investigate the quantitative relationship between **2TD** and ClO^-, absorption and fluorescence titration experiments were conducted in ~100% aqueous solution (DMSO/H_2O, 1/99, v/v) under the conditions with the concentration of **2TD** (10 μM) and variable ClO^- concentrations from 0 to 20 μM. As indicated in Fig. 2a, 2TD displayed a decreasing absorption peak at 378 nm and an emerging peak at 350 nm gradually enhanced with increasing ClO^-, suggesting the occurrence of an oxidation reaction between **2TD** and ClO^-. Meanwhile, as demonstrated in Fig. 2b, the fluorescence intensity at 423 nm enhanced greatly with the continued increase of ClO^-, and a 23-fold enhancement is observed when the amount of ClO^- concentration reached around 10 μM, which accompanied by the Φ_F increase from 12.47% to 20.09%. It is worth noting that the emission intensity increases slowly and gradually as the continuing ClO^- concentration increases, and reaches equilibrium until 10 μM ClO^-, instead of the sharp linear enhancement, implying that the reaction mole ratio between **2TD** and ClO^- is 1:1. Besides, this 1:1 stoichiometric mole ratio is also confirmed by Job's plot analysis (Fig. S6). Moreover, seen from Fig. 2c, the emission intensity (423 nm) showed an excellent linearity related to the ClO^- concentration (0–10 μM) ($R^2 = 0.993$), along with a highly sensitive color change, and the obtained detection limit (DL) was 8.3 nM based on 3σ/k [56], superior to that of the previously reported [57–61]. These illustrated that sensor **2TD** shows excellent capability for sensitively and quantitatively determining ClO^- in ~100% aqueous solution.

3.3. Sensing mechanism and DFT studies

The sensor **2TD** has no fluorescence ascribing to the isomerization of C═N, which is a predominant decay process of excited states [12,62]. When treated with the high oxidizing ability of ClO^-, it will bring out the interrupting hydrazone bond in **2TD** under the combined action of H_2O molecules, **DAMN** can be removed and accompanied by the generation of fluorophore **2T-CHO**, thus the blue fluorescence switched on

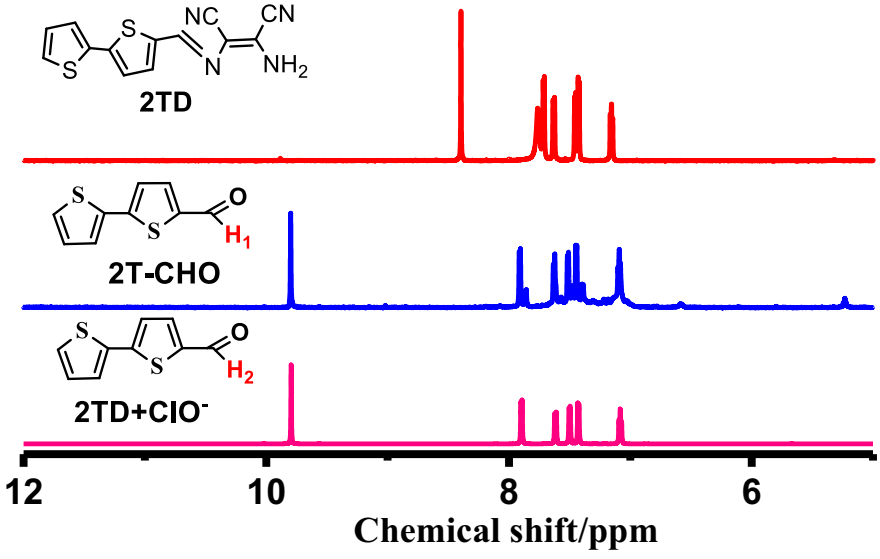

Fig. 3. ^1H NMR spectra of free **2TD**, **2TD** treated with ClO^- (**2TD** + ClO^-) and free **2T-CHO** in DMSO-d_6.

(Scheme 2), which is similar to those previously reported sensors [13,63,64].

The ^{1}H NMR spectra were firstly performed to investigate the reaction mechanism of chemosensor **2TD** with ClO^-. As presented in Fig. 3, after treating with ClO^-, a new singlet proton peak emerged at 10.31 ppm was assigned to the aldehyde (HC=O) proton signal, implying the production of cleavage product aldehyde. It was interesting to note that the ^{1}H NMR spectrum of the sensing system (**2TD**-ClO^-) was identified to that of **2T-CHO**. Subsequently, the HRMS (Fig. S7) showed that after **2TD** was treated with ClO^-, a distinct mass peak at *m/z* 191.9481 (calcd: 191.9460) was observed that is assigned to the expected product aldehyde $[M-2H]^-$. In addition, this reaction product was further supported by FTIR spectra (Fig. S8). When **2TD** treated with ClO^-, the NH_2 and C≡N stretching bands at 3455, 3302 cm^{-1} and 2207 cm^{-1} completely disappeared, accompanied by a new strong typical peak emerged at 1650 cm^{-1} corresponding to an aldehyde (HC=O) group. These proofs strongly proved the reaction mechanism that was the ClO^--provoked oxidation-hydrolysis reaction and formation of bithiophene aldehyde.

Subsequently, to further study the optical properties of **2TD** and **2T-CHO**, the TD-DFT studies were used to calculate the frontier molecular orbitals of **2TD** and **2T-CHO**, as depicted in Fig. 4. The highest occupied molecular orbital (HOMO) and the lowest unoccupied molecular orbital (LUMO) of **2T-CHO** are located on the entire molecular skeleton. However, the HOMO of **2TD** was spread over the diaminomaleonitrile and bithiophene units within the π-conjugated configuration, whereas its LUMO was located on the **DAMN** moiety. However, when **2TD** was transformed to **2T-CHO**, the ground state energy gap of **2TD** (3.024 eV) was lower than that of **2T-CHO** (3.697 eV), indicating that a strong ICT occurred throughout the π-conjugated structure of **2TD**. In addition, the absorption peak at 343 nm of **2T-CHO** was well consistent with the experimental data of 354 nm.

3.4. Time response and pH study

The ClO^- is well-known to have a quite short lifetime in biological applications, therefore, the fast-response time for real-time detection was highly desired. The influence of time on the fluorescence intensity (423 nm) change of **2TD** (10 μM) in the absence and presence of 2.0 equiv. of ClO^- was examined in ~100% aqueous solution ($DMSO/H_2O$, 1/99, v/v). The fluorescence intensity at 423 nm of the **2TD** showed no significant variation with increasing time up to 12 days, along with no distinct solution color change (Fig. S9), suggesting sensor **2TD** in the solution had excellent stability. Fig. 5a revealed that after treated with ClO^-, a significantly enhanced fluorescence was displayed, and the observed fluorescent signals arrived at the maximum and plateaued as ultra-fast as 25 s, confirmed the sensor **2TD** was capable of realizing its practical application in real-time detection of cellular ClO^-.

The pH range usually affects the detection accuracy of a chemosensor. Thus, it is great essential to study pH effects on identification of ClO^-. As shown in Fig. 5b, almost no perceptible effects on the fluorescence intensity at 423 nm of sensor **2TD** during a wide pH range 1–13, implied that no disturbance from the variation of pH. When treated with ClO^-, the fluorescence intensity at 423 nm dramatically enhanced and kept stable within the wide pH 7–11, which may be explained by that the reaction is completely transformed to the ICT

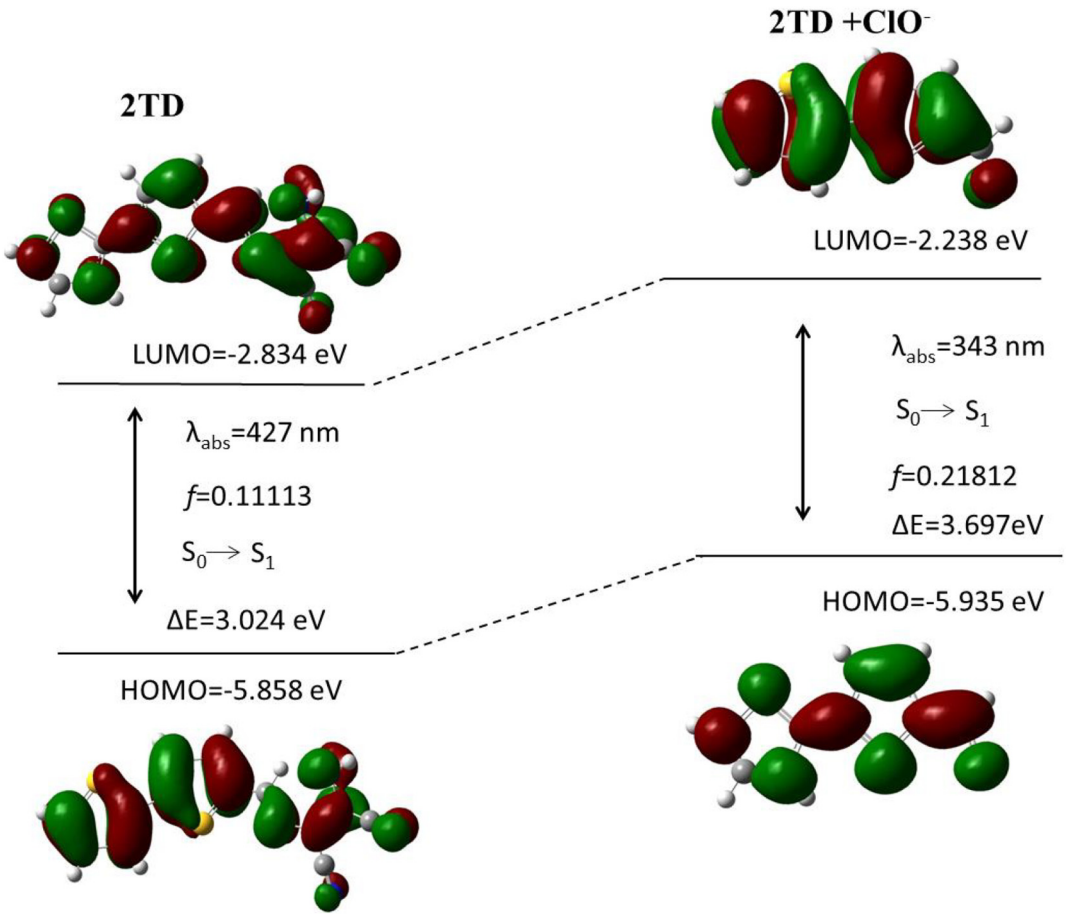

Fig. 4. The investigated molecular orbitals of **2TD** and **2T-CHO**.

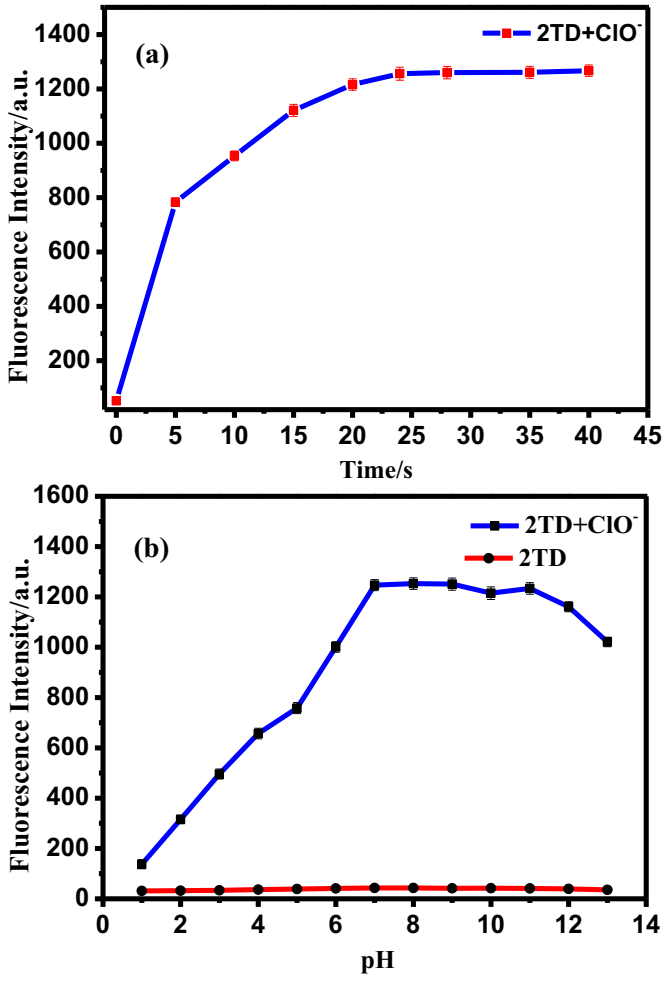

Fig. 5. The influence of time (a) or pH (b) on the fluorescence intensity (423 nm) change of **2TD** (10 μM) in the absence and presence of 2.0 equiv. of ClO^-.

fluorescent molecule **2T-CHO**. While, with the increase of alkalinity (pH 11–13), the fluorescence intensity at 423 nm decreased obviously, which may be attributed to the hydrolysis reaction and the stronger oxidation properties of the ClO^- under the acidic condition [65]. Therefore, the investigated results revealed that sensor **2TD** can be suitable for biological and pathological tests (pH 7–11).

3.5. Real water sample test

To validate the practicality, the sensor **2TD** was applied for detecting and monitoring the levels of ClO^- in real water samples using standard addition method. With the adding an identified amount of standard ClO^- (5.0 and 10.0 μM) to each sample, the fluorescence spectra and their detection reliabilities was presented in Fig. S10 and Table 1, respectively. The high recoveries for the addition ranged from 98.2% to 101.8% and the RSD values were calculated below 3%, which are favorably compared with those obtained by standard methods in the literature [66,67]. These satisfactory results demonstrated that sensor **2TD** showed good reliability to sensitively detect and monitor trace levels of ClO^- in practical water samples for practical applications.

Table 1
Detecting ClO^- in four water samples.

Sample	Added (μM)	Detect ($\bar{x}$ ± SD) (μM)	Recovery (%)	Relative error (%)	RSD (%)
Tap water	5.0	4.91 ± 0.12	98.2	1.8	2.4
	10.0	10.16 ± 0.15	101.6	1.6	1.5
River water	5.0	4.95 ± 0.11	99	1	2.2
	10.0	10.15 ± 0.14	101.5	1.5	1.4
Distilled water	5.0	4.92 ± 0.11	98.4	1.6	2.2
	10.0	10.17 ± 0.14	101.7	1.7	1.4
Lake water of Ji'nan Garden Expo	5.0	5.09 ± 0.12	101.8	1.8	2.4
	10.0	10.14 ± 0.15	101.4	1.4	1.5

3.6. Bio-imaging of ClO^- in living cells

To investigate its biological application, the fluorescence imaging of **2TD** for detecting ClO^- in live cells was performed. Before imaging, the cytotoxic behaviour of **2TD** was tested through the MTT assay with HeLa cells for 24 h (Fig. 6a). The results showed that the 93% HeLa cells can still keep alive at 30 μM, indicated that the sensor **2TD** has no obvious cytotoxicity and was relatively safe in bioimaging application. The cell imaging test was then performed. The HeLa cells only incubated with 10 μM **2TD** for 60 min caused almost no observed fluorescence (Fig. 6b, c). By contrast, when the HeLa cells were treated with ClO^- (30 μM) for 10 min, a prominent blue fluorescence was clearly found (Fig. 6d). And the quantification of fluorescence intensity was calculated to be 25.56 a.u., which is ca. 21-fold enhancement compared with that of **2TD** (Fig. S11). Therefore, the cell imaging experimental results confirmed that sensor **2TD** was capable of imaging ClO^- in living HeLa cells.

3.7. Application as solid-state sensor for sensing ClO^-

To further explore its application for visual, real-time and on-site monitoring ClO^- in environmental system, the usefulness of the **2TD** as a solid-state sensor for sensing ClO^- in coated filter papers was tested (SI). When the **2TD**-loaded test strips were immersed into water containing an increasing amount of ClO^- for several minutes, rapid and significant visual color changes were clearly detected by naked eyes (Fig. 7), confirming that **2TD** could be used as a cost-effective solid-state sensor for the rapid and convenient sensing ClO^- with great sensitivity in practical applications.

3.8. Application as fluorescent display material

Interestingly, due to the above good fluorescent sensing performance, sensor **2TD** could serve as a rewritable small-molecular smart fluorescent display material. As displayed in Fig. 8a, when the sensor **2TD** (10 μM) was loaded into a pen without any modification and was used to write text, Chinese characters and patterns on the filter papers, obvious yellow text, characters (such as "Qilu University of Technology") and patterns on the handwritten filter paper can be easily and clearly detected under sunlight. As shown in Fig. 8b, when writing on the **2TD**-based filter papers with a pen loaded ClO^- aqueous solution (10 μM), bright blue fluorescent text, characters (such as "Qilu University of Technology") and fluorescent patterns on the handwritten filter paper were obviously observed under 365 nm UV light, which showed significant color change for ClO^- and displayed highly distinct from the background, indicating that **2TD** could be used as a conveniently sensing ClO^- test tool and as a good fluorescent display material. Therefore, developing this type fluorescent display material is more advantageous and convenient for sensing ClO^-.

3.9. Comparison with other sensors

Compared with previous ClO^--specific fluorescent sensors (Table S1) [68–74], our developed sensor **2TD** showed several advantages: (i) simple structure and worked in ~100% aqueous media with dual responses; (ii) ultra-sensitive (8.3 nM) and ultra-rapid (25 s) detecting and monitoring trace levels of ClO^-; (iii) multiple applications in real water sample analysis, test strip, cell imaging,

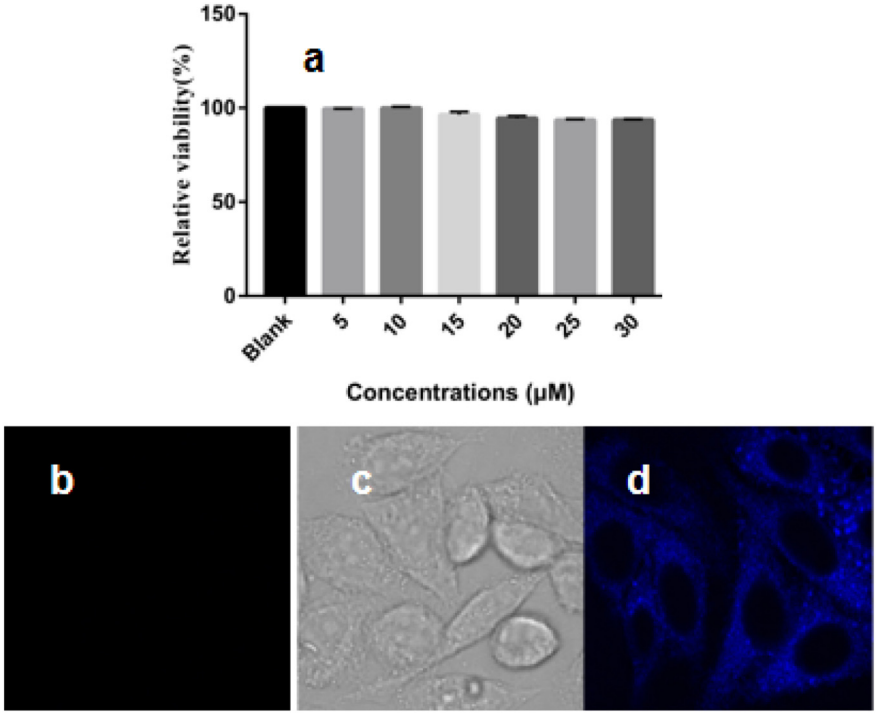

Fig. 6. (a) Cell viability of cells treated with varied **2TD** for 24 h; Fluorescence images of HeLa cells treated with 10 μM **2TD** (b, c), and further treated with 30 μM ClO^- for 10 min (d). λ_{ex} = 405 nm, λ_{em} = 430–470 nm.

and fluorescent display, which provided proofs for good idea of integrating multiple functions into one sensor molecule. Although two sensors were reported with shorter reaction time, the DL was higher [71,72]. It indicated that our synthesized sensor could be used as a rapid and sensitive analytical method for detecting ClO^-.

4. Conclusions

In summary, a new bithiophene-based sensor **2TD** was successfully designed and synthesized, which showed unique optical selectivity for ClO^- in ~100% aqueous solution with colorimetric and fluorescent turn-on dual responses. Sensor **2TD** for ClO^- sensing showed ultra-fast response, wide pH working range, ultrasensitivity, as well as strong anti-interference capability. The sensing mechanism was proposed and was well confirmed by optical spectra, ^1H NMR, HRMS, FTIR and TD-DFT studies. Colorimetric test strips demonstrated that the **2TD** can be utilized as a cost-effective and efficient solid-state sensor for rapid and convenient detecting ClO^- with great sensitivity in practical applications. Sensor **2TD** has excellent practicability of great water solubility, negligible cytotoxicity and good biocompatibility, and applied to sensitively monitor ClO^- in environmental samples as well as the living HeLa cells. Moreover, the sensor **2TD** could be utilized as a good fluorescent display material and an efficient ClO^--sensing test tool.

CRediT authorship contribution statement

Chunpeng Li: Conceptualization, Data curation, Software, Investigation, Writing - original draft. **Pengcheng Yin:** Conceptualization, Data curation, Formal analysis. **Tianduo Li:** Resources, Formal analysis, Writing - review & editing. **Tao Wei:** Formal analysis, Writing - review & editing. **Tingting Hu:** Writing - review & editing. **Jianbin Chen:** Writing - review & editing. **Xuyang Qin:** Writing - review & editing. **Qingfen Niu:** Resources, Writing - review & editing, Supervision, Data curation.

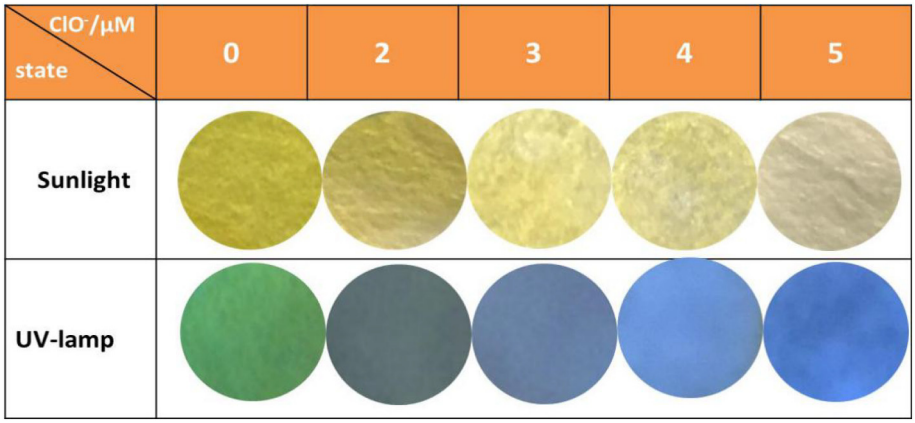

Fig. 7. Photograph of test strips of **2TD** with increasing ClO^- concentrations.

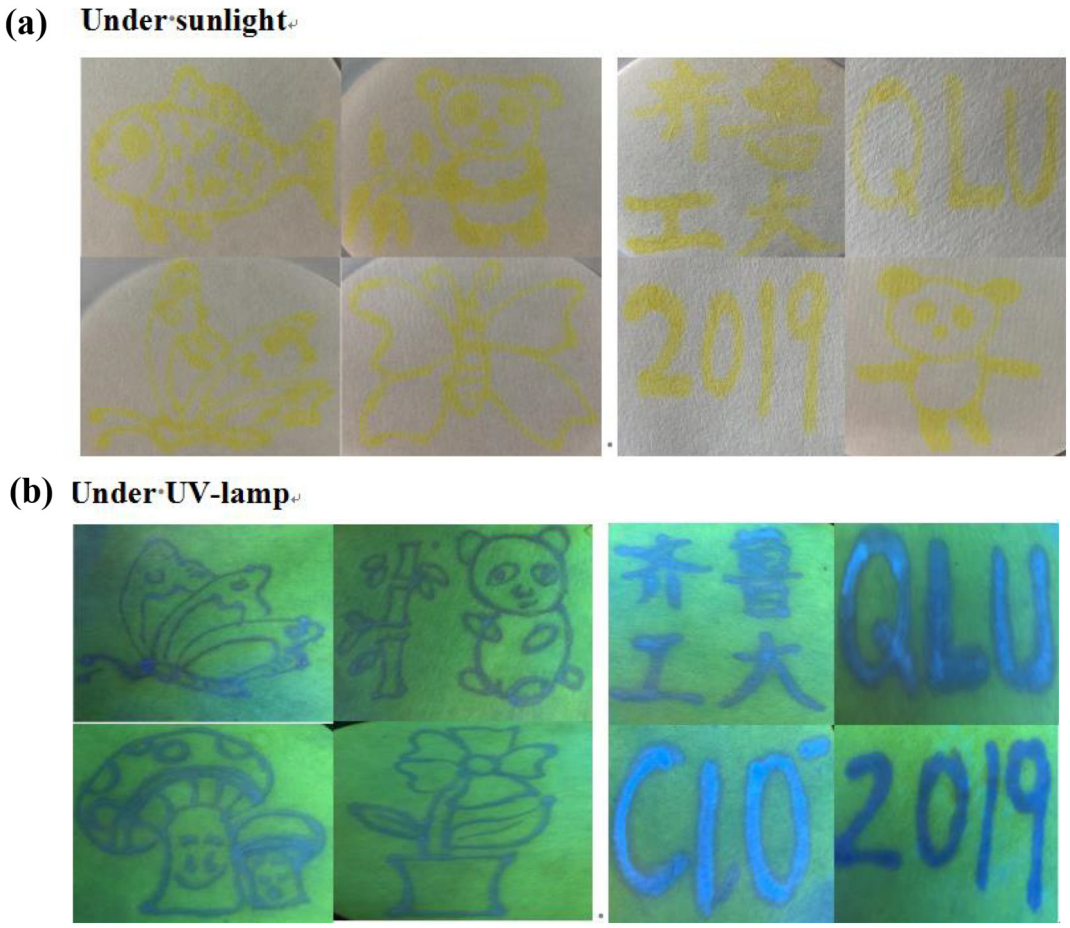

Fig. 8. (a) The photographic images of the colorimetric patterns/text written on a **2TD** (10 μM) loaded filter paper under sunlight; (b) the photographic images of the fluorescent patterns/text written on a **2TD**-loaded filter paper using the ClO^- aqueous solution (10 μM) under 365 illumination.

Declaration of competing interest

The authors declare no competing financial interest.

Acknowledgments

We greatly appreciate financial support from the National Natural Science Foundation of China (21776143, 21801144, 51702178, 21376125), the Jinan Science & Technology Bureau (2019GXRC021), the Natural Science Foundation of Shandong Province (ZR2017LB009), the Program for College Students' Innovation and Entrepreneurship Training of Shandong Province (S201910431035), the Youth Innovative Talents Recruitment and Cultivation Program of Shandong Higher Education, and the Program for Scientific Research Innovation Team in Colleges and Universities of Shandong Province.

Appendix A. Supplementary data

Supplementary data to this article can be found online at https://doi.org/10.1016/j.molliq.2020.114396.

References

[1] B. D'Autreaux, M.B. Toledano, ROS as signalling molecules: mechanisms that generate specificity in ROS homeostasis, Nat. Rev. Mol. Cell. Biol. 8 (2007) 813–824.
[2] C.C. Winterbourn, Reconciling the chemistry and biology of reactive oxygen species, Nat. Chem. Biol. 4 (2008) 278–286.
[3] Y. Koide, Y. Urano, S. Kenmoku, H. Kojima, T. Nagano, Design and synthesis of fluorescent probes for selective detection of highly reactive oxygen species in mitochondria of living cells, J. Am. Chem. Soc. 129 (2007) 10324–10325.
[4] X. Chen, X. Tian, I. Shin, J. Yoon, ChemInform abstract: fluorescent and luminescent probes for detection of reactive oxygen and nitrogen species, Chem. Soc. Rev. 40 (2011) 4783–4804.
[5] Y. Koide, Y. Urano, K. Hanaoka, T. Terai, T. Nagano, Development of an Si-rhodamine-based far-red to near-infrared fluorescence probe selective for hypochlorous acid and its applications for biological imaging, J. Am. Chem. Soc. 133 (2011) 5680–5682.
[6] Q.A. Best, N. Sattenapally, D.J. Dyer, C.N. Scott, M.E. McCarroll, pH-dependent si-fluorescein hypochlorous acid fluorescent probe: spirocycle ring-opening and excess hypochlorous acid-induced chlorination, J. Am. Chem. Soc. 135 (2013) 13365–13370.
[7] Y. Liu, K. Li, M.Y. Wu, Y.H. Liu, Y.M. Xie, X.Q. Yu, A mitochondria-targeted colorimetric and ratiometric fluorescent probe for biological SO_2 derivatives in living cells, Chem. Commun. 51 (2015) 10236–10239.
[8] T. Nagano, Bioimaging probes for reactive oxygen species and reactive nitrogen species, J. Clin. Biochem. Nutr. 45 (2009) 111–124.
[9] B.C. Dickinson, C.J. Chang, Chemistry and biology of reactive oxygen species in signaling or stress responses, Nat. Chem. Biol. 7 (2011) 504–511.
[10] N. Güngör, A.M. Knaapen, A. Munnia, M. Peluso, G.R. Haenen, R.K. Chiu, R.W.L. Godschalk, F.J. Van Schooten, Genotoxic effects of neutrophils and hypochlorous acid, Mutagenesis 25 (2010) 149–154.
[11] W.A. Rutala, D.J. Weber, Uses of inorganic hypochlorite (bleach) in health-care facilities, Clin. Microbiol. Rev. 10 (1997) 597–610.
[12] Y. Wang, J. Xia, J. Han, X. Bao, Y. Li, X. Tang, L. Ni, L. Wang, M. Gao, A fast-responsive fluorescent probe based on BODIPY dye for sensitive detection of hypochlorite and its application in real water samples, Talanta 161 (2016) 847–853.
[13] X. Tang, Z. Zhu, R. Liu, Y. Tang, A novel ratiometric and colorimetric fluorescent probe for hypochlorite based on cyanobiphenyl and its applications, Spectrochim. Acta A 219 (2019) 576–581.
[14] M.K. Shigenaga, T.M. Hagen, B.N. Ames, Oxidative damage and mitochondrial decay in aging, Proc. Natl. Acad. Sci. 91 (1994) 10771–10778.

[15] E. Malle, T. Buch, H.J. Grone, Myeloperoxidase in kidney disease, Kidney Int. 64 (2003) 1956–1967.
[16] D.I. Pattison, M.J. Davies, Evidence for rapid inter-and intramolecular chlorine transfer reactions of histamine and carnosine chloramines: implications for the prevention of hypochlorous-acid-mediated damage, Biochemistry 45 (2006) 8152–8162.
[17] P.D. Ray, B.W. Huang, Y. Tsuji, Reactive oxygen species (ROS) homeostasis and redox regulation in cellular signaling, Cell. Signal. 24 (2012) 981–990.
[18] K. Żamojć, M. Zdrowowicz, D. Jacewicz, D. Wyrzykowski, L. Chmurzyński, Fluorescent and luminescent probes for monitoring hydroxyl radical under biological conditions, Crit. Rev. Anal. Chem. 46 (2016) 160.
[19] H. Zhang, L.Z. Xu, W.Q. Chen, J. Huang, C.S. Huang, J.R. Sheng, X.Z. Song, Simultaneous discrimination of cysteine, homocysteine, glutathione, and H_2S in living cells through a multisignal combination strategy, Anal. Chem. 91 (2019) 1904–1911.
[20] L. Yuan, W. Lin, K. Zheng, S. Zhu, FRET-based small-molecule fluorescent probes: rational design and bioimaging applications, Acc. Chem. Res. 46 (2013) 1462–1473.
[21] P.A. Gale, C. Caltagirone, Anion sensing by small molecules and molecular ensembles, Chem. Soc. Rev. 44 (2015) 4212–4227.
[22] D. Qu, Q. Wang, Q. Zhang, X. Ma, H. Tian, Photoresponsive host-guest functional systems, Chem. Rev. 115 (2015) 7543–7588.
[23] Y. Tang, D. Lee, J. Wang, G. Li, J. Yu, W. Lin, J. Yoon, Development of fluorescent probes based on protection-deprotection of the key functional groups for biological imaging, Chem. Soc. Rev. 44 (2015) 5003–5015.
[24] D. Wu, L.Y. Chen, Q.L. Xu, X.Q. Chen, J.Y. Yoon, Design principles, sensing mechanisms, and applications of highly specific fluorescent probes for HOCl/OCl^-, Acc. Chem. Res. 52 (2019) 2158–2168.
[25] P. Wei, W. Yuan, F. Xue, W. Zhou, R. Li, D. Zhang, T. Yi, Deformylation reaction-based probe for in vivo imaging of HOCl, Chem. Sci. 9 (2018) 495–501.
[26] D. Shi, S. Chen, B. Dong, Y. Zhang, C. Sheng, T.D. James, Y. Guo, Evaluation of HOCl-generating anticancer agents by an ultrasensitive dual-mode fluorescent probe, Chem. Sci. 10 (2019) 3715–3722.
[27] J.-T. Hou, H.S. Kim, C. Duan, M.S. Ji, S. Wang, L. Zeng, W. Ren, J.S. Kim, A ratiometric fluorescent probe for detecting hypochlorite in the endoplasmic reticulum, Chem. Commun. 55 (2019) 2533–2536.
[28] C. Duan, M. Won, P. Verwilst, J.C. Xu, S. Kim, L.T. Zeng, J.S. Kim, Produced HClO in zebrafish and mice using a bright, photostable ratiometric fluorescent probe, Anal. Chem. 91 (2019) 4172–4178.
[29] H. Feng, Z.Q. Zhang, Q.T. Meng, H.M. Jia, Y. Wang, R. Zhang, Rapid response fluorescence probe enabled in vivo diagnosis and assessing treatment response of hypochlorous acid-mediated rheumatoid arthritis, Adv. Sci. 5 (2018), 1800397, .
[30] Z. Mao, M. Ye, W. Hu, X. Ye, Y. Wang, H. Zhang, C. Li, Z. Liu, Design of a ratiometric two-photon probe for imaging of hypochlorous acid (HClO) in wounded tissues, Chem. Sci. 9 (2018) 6035–6040.
[31] Q. Yuan, Z.M. Zhao, Y.R. Zhang, L. Su, J.Y. Miao, B.X. Zhao, A lysosome-targeted ratiometric fluorescent probe for detection of hypochlorous acid in living cells, Sensors Actuators B Chem. 247 (2017) 736–741.
[32] R. Zhang, J. Zhao, G. Han, Z. Liu, C. Liu, C. Zhang, B. Liu, C. Jiang, R. Liu, T. Zhao, M.Y. Han, Z. Zhang, Real-time discrimination and versatile profiling of spontaneous reactive oxygen species in living organisms with a single fluorescent probe, J. Am. Chem. Soc. 138 (2016) 3769–3778.
[33] J.F. Li, P.F. Li, F.L. Huo, C.X. Yin, T. Liu, J.B. Chao, Y.B. Zhang, Ratiometric fluorescent probes for ClO^- and in vivo applications, Dyes Pigments 130 (2016) 209–215.
[34] L. He, Y. Zhang, H.Q. Xiong, J.P. Wang, Y.N. Geng, B.H. Wang, Y.G. Wang, Z.G. Yang, X.Z. Song, A ratiometric flavone-based fluorescent probe for hypochlorous acid detection with large Stokes shift and long-wavelength emission, Dyes Pigments 166 (2019) 390–394.
[35] B. Zhang, X. Yang, R. Zhang, Y. Liu, X. Ren, M. Xian, Y. Ye, Y. Zhao, Lysosomal-targeted two-photon fluorescent probe to sense hypochlorous acid in live cell, Anal. Chem. 89 (2017) 10384–10390.
[36] X. Xie, T. Wu, X. Wang, Y. Li, K.Y. Wang, Z.W. Zhao, X.Y. Jiao, B. Tang, A two-photon fluorescent probe for ratiometric visualization of hypochlorous acid in live cells and animals based on a selenide oxidation/elimination tandem reaction, Chem. Commun. 54 (2018) 11965–11968.
[37] J. Wang, T. Wei, F. Ma, T. Li, Q. Niu, A novel fluorescent and colorimetric dual-channel sensor for the fast, reversible and simultaneous detection of Fe^{3+} and Cu^{2+} based on terthiophene derivative with high sensitivity and selectivity, J. Photochem. Photobiol. A 383 (2019), 111982, .
[38] Z. Guo, T. Hu, X. Wang, T. Sun, T. Li, Q. Niu, Highly sensitive and selective fluorescent sensor for visual detection of Cu^{2+} in water and food samples based on oligothiophene derivative, J. Photochem. Photobiol. A 371 (2019) 50–58.
[39] J. Wang, Q. Niu, T. Hu, T. Wei, T. Li, A new phenothiazine-based sensor for highly selective, ultrafast, ratiometric fluorescence and colorimetric sensing of Hg^{2+}: applications to bioimaging in living cells and test strips, J. Photochem. Photobiol. A 384 (2019), 112036, .
[40] Z. Zuo, X. Song, D. Guo, Z. Guo, Q. Niu, A dual responsive colorimetric/fluorescent turn-on sensor for highly selective, sensitive and fast detection of Fe^{3+} ions and its applications, J. Photochem. Photobiol. A 382 (2019), 111876, .
[41] Z. Guo, Q. Niu, T. Li, E. Wang, Highly chemoselective colorimetric/fluorometric dual-channel sensor with fast response and good reversibility for the selective and sensitive detection of Cu^{2+}, Tetrahedron 75 (2019) 3982–3992.
[42] Z. Guo, Q. Niu, T. Li, T. Sun, H. Chi, A fast, highly selective and sensitive colorimetric and fluorescent sensor for Cu^{2+} and its application in real water and food samples, Spectrochim. Acta A 213 (2019) 97–103.
[43] P. Yin, Q. Niu, Q. Yang, L. Lan, T. Li, A new "naked-eye" colorimetric and ratiometric fluorescent sensor for imaging Hg^{2+} in living cells, Tetrahedron 75 (2019), 130687.
[44] P. Yin, Q. Niu, T. Wei, T. Li, Y. Li, Q. Yang, A new thiophene-based dual functional chemosensor for ultrasensitive colorimetric detection of Cu^{2+} in aqueous solution and highly selective fluorimetric detection of Al^{3+} in living cells, J. Photochem. Photobiol. A 389 (2020), 112249, .
[45] C. Li, Q. Niu, J. Wang, T. Wei, T. Li, J. Chen, X. Qin, Q. Yang, Bithiophene-based fluorescent sensor for highly sensitive and ultrarapid detection of Hg^{2+} in water, seafood, urine and live cells, Spectrochim. Acta A 233 (2020), 118208, .
[46] C. Li, Q. Niu, T. Li, T. Wei, T. Hu, J. Chen, X. Qin, L. Yang, A novel dual-function bithiophene-Meldrum's acid based chemosensor for highly sensitive, colorimetric and fluorimetric detection of cyanide and hypochlorite and its applications, Dyes Pigments 180 (2020), 108459, .
[47] Z. Guo, Q. Niu, Q. Yang, T. Li, H. Chi, A highly selective and sensitive dual-mode sensor for colorimetric and turn-on fluorescent detection of cyanide in water, agro-products and living cells, Anal. Chim. Acta 1065 (2019) 113–123.
[48] Z. Guo, T. Hu, T. Sun, T. Li, H. Chi, Q. Niu, A colorimetric and fluorometric oligothiophene-indenedione-based sensor for rapid and highly sensitive detection of cyanide in real samples and bioimaging in living cells, Dyes Pigments 163 (2019) 667–674.
[49] Z. Guo, Q. Niu, Q. Yang, T. Li, T. Wei, L. Yang, J. Chen, X. Qin, New "naked-eye" colori/flfluorimetric "turn-on" chemosensor: ultrafast and ultrasensitive detection of hydrazine in ~100% aqueous solution and its bio-imaging in living cells, Anal. Chim. Acta 1123 (2020) 64–72.
[50] J. Wang, Q. Niu, T. Wei, T. Li, T. Hu, J. Chen, X. Qin, Q. Yang, L. Yang, Novel phenothiazine-based fast-responsive colori/fluorimetric sensor for highly sensitive, selective and reversible detection of Cu^{2+} in real water samples and its application as an efficient solid-state sensor, Microchem. J. 157 (2020), 104990, .
[51] P. Yin, Q. Niu, T. Li, T. Wei, J. Chen, X. Qin, A new aggregation-induced emission active red-emitting flfluorescent sensor for ultrarapidly, selectively and sensitively detecting hydrazine and its multiple applications, J. Mol. Liq. 316 (2020), 113845, .
[52] Q. Niu, Y. Lu, H. Sun, X. Li, X. Tao, Novel phenyl-oligothiophene derivatives containing acetylenic spacers for thin film materials: synthesis, photophysical and morphology properties, Dyes Pigments 97 (2013) 184–197.
[53] C.G. Wu, M.F. Chung, H.H.G. Tsai, C.J. Tan, S.C. Chen, C.H. Chang, T.W. Shih, Fluorene-containing organic photosensitizers for dye-sensitized solar cells, ChemPlusChem 77 (2012) 832–843.
[54] Z. Wang, X. Teng, C. Lu, Orderly arranged fluorescence dyes as a highly efficient chemiluminescence resonance energy transfer probe for peroxynitrite, Anal. Chem. 87 (2015) 3412–3418.
[55] Y. Fenga, S. Li, D. Li, Q. Wang, P. Ning, M. Chen, X. Tian, X. Wang, Rational design of a diaminomaleonitrile-based mitochondria–targeted two-photon fluorescent probe for hypochlorite in vivo: solvent-independent and high selectivity over Cu^{2+}, Sensors Actuators B 254 (2018) 282–290.
[56] Y. Zhou, K.N. Bobba, X.W. Lv, D. Yang, N. Velusamy, J.F. Zhang, S. Bhuniya, A biotinylated piperazine-rhodol derivative: a 'turn-on' probe for nitroreductase triggered hypoxia imaging, Analyst 142 (2017) 345–350.
[57] F. Tian, Y. Jia, Y. Zhang, W. Song, G. Zhao, Z. Qu, A HClO-specific near-infrared fluorescent probe for determination of myeloperoxidase activity and imaging mitochondrial HClO in living cells, Biosens. Bioelectron. 86 (2016) 68–74.
[58] X. Jiao, K. Huang, S. He, C. Liu, L. Zhao, X. Zeng, A mitochondria-targeted near-infrared fluorescent probe with a large Stokes shift for real-time detection of hypochlorous acid, Org. Biomol. Chem. 17 (2019) 108–114.
[59] B. Shen, Y. Qian, Z. Qi, C. Lu, Q. Sun, X. Xia, Y. Cui, Near-infrared BODIPY-based two-photon ClO^- probe based on thiosemicarbazide desulfurization reaction: naked-eye detection and mitochondrial imaging, J. Mater. Chem. B 5 (2017) 5854–5861.
[60] L. Chen, S.J. Park, D. Wu, H.M. Kim, J. Yoon, A two-photon ESIPT based fluorescence probe for specific detection of hypochlorite, Dyes Pigments 158 (2018) 526–532.
[61] Y. Zhang, L. Ma, C. Tang, S. Pan, D. Shi, S. Wang, M. Li, Y. Guo, A highly sensitive and rapidly responding fluorescent probe based on a rhodol fluorophore for imaging endogenous hypochlorite in living mice, J. Mater. Chem. B 6 (2018) 725–731.
[62] X. Cheng, H. Jia, T. Long, J. Feng, J. Qin, Z. Li, A "turn-on" fluorescent probe for hypochlorous acid: convenient synthesis, good sensing performance, and a new design strategy by the removal of C=N isomerization, Chem. Commun. 47 (2011) 11978–11980.
[63] X.J. Zhao, Y.R. Jiang, Y.X. Chen, B.Q. Yang, Y.T. Li, Z.H. Liu, C. Liu, A new "off-on" NIR fluorescence probe for determination and bio-imaging of mitochondrial hypochlorite in living cells and zebrafish, Spectrochim. Acta A 219 (2019) 509–516.
[64] Y. Ning, J. Cui, Y. Lu, X. Wang, C. Xiao, S. Wu, J. Li, Y. Zhang, De novo design and synthesis of a novel colorimetric fluorescent probe based on naphthalenone scaffold for selective detection of hypochlorite and its application in living cells, Sensors Actuators B Chem. 269 (2018) 322–330.
[65] X. Tang, Z. Zhu, Y. Wang, J. Han, L. Ni, H. Zhang, J. Li, Y. Mao, A cyanobiphenyl based fluorescent probe for rapid and specifific detection of hypochlorite and its bioimaging applications, Sensors Actuators B Chem. 262 (2018) 57–63.
[66] H. Pan, Y. Liu, S. Liu, Z. Ou, H. Chen, H. Li, A dual-function colorimetric probe based on cyanine-carbazole dyad for highly sensitive recognition of cyanide and hypochlorite in aqueous media, Talanta 202 (2019) 329–339.
[67] Z.C. Wang, Q.H. Zhang, J.W. Liu, R. Sui, Y.H. Li, Y. Li, X.F. Zhang, H.B. Yu, K. Jing, M.Y. Zhang, Y. Xiao, A twist six-membered rhodamine-based fluorescent probe for hypochlorite detection in water and lysosomes of living cells, Anal. Chim. Acta 1082 (2019) 116–125.
[68] H. Yu, Y. Wu, Y. Hu, X.D. Gao, Q. Liang, J. Xu, S.J. Shao, Dual-functional fluorescent probe responds to hypochlorous acid and SO_2 derivatives with different fluorescence signals, Talanta 165 (2017) 625–631.
[69] Z.W. Ma, X.P. Chen, C.C. Wang, Q.J. Lv, A novel ratiometric fluorescence probe for hypochlorite detection and its application in cell imaging, J. Mol. Struct. 1221 (2020), 128812, .

[70] V.N. Nguyen, S. Heo, S. Kim, K.M.K. Swamy, J. Ha, S. Park, J. Yoon, A thiocoumarin-based turn-on fluorescent probe for hypochlorite detection and its application to live-cell imaging, Sensors Actuators B Chem. 317 (2020), 128213, .
[71] X. Tang, Z. Zhu, Y. Wang, J. Han, L. Ni, H.Q. Zhang, J. Li, Y.L. Mao, A cyanobiphenyl based fluorescent probe for rapid and specific detection of hypochlorite and its bio-imaging applications, Sensors Actuators B Chem. 262 (2018) 57–63.
[72] Y.L. Jiang, S. Zhang, B.X. Wang, T. Qian, C. Jin, S.S. Wu, J. Shen, Novel triphenylamine-based fluorescent probe for specific detection and bioimaging of OCl^-, Tetrahedron 74 (2018) 5733–5738.
[73] Z.W. Ma, X. Wang, C.C. Wang, X.Q. Chen, Q.J. Lv, A sensitiveand selectivefluorescence probe for detectionof hypochlorite (OCl^-) and its bioimaging in live cells, Spectrochim. Acta A 213 (2019) 370–374.
[74] X.Z. Song, B.L. Dong, X.Q. Kong, C. Wang, N. Zhang, W.Y. Lin, Construction of a ratiometric fluorescent probe with an extremely large emission shift for imaging hypochlorite in living cells, Spectrochim. Acta A 188 (2018) 394–399.